The Journal of Immunology

C-Type Lectin Receptor CD23 Is Required for Host Defense against *Candida albicans* and *Aspergillus fumigatus* Infection

Yahui Guo, Qing Chang, Liqing Cheng, Sihan Xiong, Xinming Jia, Xin Lin and Xueqiang Zhao

J Immunol published online 5 September 2018
http://www.jimmunol.org/content/early/2018/09/04/jimmunol.1800620

Supplementary Material **http://www.jimmunol.org/content/suppl/2018/09/04/jimmunol.1800620.DCSupplemental**

The Journal of Immunology is published twice each month by
The American Association of Immunologists, Inc.,
1451 Rockville Pike, Suite 650, Rockville, MD 20852

Print ISSN: 0022-1767 Online ISSN: 1550-6606.

Published September 5, 2018, doi:10.4049/jimmunol.1800620

C-Type Lectin Receptor CD23 Is Required for Host Defense against *Candida albicans* and *Aspergillus fumigatus* Infection

Yahui Guo,* Qing Chang,* Liqing Cheng,*,† Sihan Xiong,*,† Xinming Jia,‡ Xin Lin,*,†,§ and Xueqiang Zhao*,§

Infection by invasive fungi, such as *Candida albicans*, *Aspergillus fumigatus*, and *Cryptococcus neoformans*, is one of the leading death causes for the increasing population of immunocompromised and immunodeficient patients. Several C-type lectin receptors (CLRs), including Dectin-1, -2, and -3 and Mincle can recognize fungal surface components and initiate the host antifungal immune responses. Nevertheless, it remains to be determined whether other CLRs are involved in antifungal immunity. Our recent study suggests that CD23 (CLEC4J), a CLR and also a well-known B cell surface marker, may function to sense *C. albicans* components in antifungal immunity. However, it is not clear how CD23 functions as a fungal pattern recognition receptor and whether the antifungal role of CD23 is specific to *C. albicans* or not. In this study, we show that CD23 can recognize both α-mannan and β-glucan from the cell wall of *C. albicans* or *A. fumigatus* but cannot recognize glucuronoxylomannan from *Cryptococcus*. Through forming a complex with FcRγ, CD23 can induce NF-κB activation. Consistently, CD23-deficient mice were highly susceptible to *C. albicans* and *A. fumigatus* but not to *C. neoformans* infection. The expression of CD23 in activated macrophages is critical for the activation of NF-κB. CD23 deficiency results in impaired expression of NF-κB–dependent genes, especially *iNOS*, which induces NO production to suppress fungal infection. Together, our studies reveal the CD23-induced signaling pathways and their roles in antifungal immunity, specifically for *C. albicans* and *A. fumigatus*, which provides the molecular basis for designing potential therapeutic agents against fungal infection. *The Journal of Immunology*, 2018, 201: 000–000.

Invasive fungal infection kills about 1.5 million people each year. *Candida albicans*, *Aspergillus fumigatus*, and *Cryptococcus neoformans* are associated with approximately 90% of all reported fungi-related death (1, 2). *C. albicans* is the most frequent fungal species isolated from infected intensive care unit patients, followed by *A. fumigatus* and then *C. neoformans* (1). In healthy individuals, these fungal species are commensal microbes. However, for the increasing population of immunocompromised and immunodeficient individuals, opportunistic fungal infection can cause severe invasive diseases, such as invasive candidiasis, aspergillosis, or cryptococcosis, which are life-threatening for these individuals (2–5).

C. albicans cell walls are composed of multiple layers of carbohydrates, including α-mannan, β-glucan, and chitin (6, 7). *A. fumigatus* cell walls are composed of melanin protein, α-(1,3)-glucan, galactosaminogalactan, galactofuran, mannan, β-glucan, and chitin (8). *C. neoformans* has been classified into three serotypes including A, D, and AD hybrid, whereas serotypes B and C have been recognized as a separate species called *Cryptococcus gattii* based on antigenic differences in the polysaccharide capsules of the fungus (9). Cryptococcal capsule is composed primarily of glucuronoxylomannan (GXM), which composes more than 90% of the capsule's polysaccharide mass (10).

Host immune cells, including macrophages and dendritic cells, recognize pathogen-associated molecular patterns via pattern recognition receptors (PRRs) that elicit the host antipathogen responses. C-type lectin receptors (CLRs), such as Dectin-1, Dectin-2, and Dectin-3, are a type of PRR recognizing pathogen-associated molecular patterns composed of polysaccharides and play pivotal roles in host defense against fungal infection (4, 7, 11–13). Genetic deficiency of Dectin-1, a representative CLR recognizing β-1,3-glucan of *C. albicans* yeast and *A. fumigatus* conidia (14, 15), did not influence the clearance of *C. neoformans* pulmonary infections (16). Dectin-2 can recognize α-mannan of *C. albicans* and *A. fumigatus* hyphae, lipophilic and mannose-capped lipoarabinomannan of *Mycobacterium tuberculosis*, and unknown components of *C. neoformans* (17–19). Dectin-3 alone, or associated with Dectin-2 to form heterodimer, senses α-mannan from *C. albicans* hyphae form (20), and Dectin-3 is also required for clearance of *C. neoformans* (21). Moreover, Dectin-3 can recognize trehalose 6,6′-dimycolate (TDM) of *M. tuberculosis* (22).

*Institute for Immunology, Tsinghua University School of Medicine, Beijing 100084, China; †Tsinghua University–Peking University Joint Center for Life Sciences, Beijing 100084, China; ‡Department of Immunology, Tongji University School of Medicine, Shanghai 200433, China; and §Beijing Key Lab for Immunological Research on Chronic Diseases, Beijing 100084, China

ORCIDs: 0000-0003-1587-4619 (Y.G.); 0000-0002-9403-0694 (S.X.); 0000-0002-7245-5560 (X.J.).

Received for publication April 30, 2018. Accepted for publication August 6, 2018.

This work was supported by grants from the National Natural Science Foundation of China (81630058 to X.L. and 31670904 and 81502460 to X.Z.) and the research fund of the Tsinghua University–Peking University Joint Center for Life Sciences (to X.L.).

Y.G., X.L., and X.Z. designed the study. Y.G., Q.C., L.C., and S.X. performed the experiments and collected and analyzed data. X.J. provided reagents and gave conceptual advice. Y.G., X.L., and X.Z. wrote the manuscript.

Address correspondence and reprint requests to Dr. Xin Lin and Dr. Xueqiang Zhao, Institute for Immunology and School of Medicine, Tsinghua University, 30 Shuangqing Road, Haidian District, Beijing 100084, China. E-mail addresses: linxin307@tsinghua.edu.cn (X.L.) and zhaoxueqiang@tsinghua.edu.cn (X.Z.)

The online version of this article contains supplemental material.

Abbreviations used in this article: BMDM, bone marrow–derived macrophage; CD23 Het, CD23 heterozygous; ChIP, chromatin immunoprecipitation; CLR, C-type lectin receptor; GMS, Gomori methenamine silver; GXM, glucuronoxylomannan; HKC, heat-killed *C .albicans*; iBMDM, immortalized BMDM; iNOS, inducible NO synthase; KO, knockout; MHC II, MHC class II; MOI, multiplicity of infection; MUT, mutant; PAS, periodic acid–Schiff; PM, peritoneal macrophage; PRR, pattern recognition receptor; ROS, reactive oxygen species; WT, wild-type.

Dectin-1, Dectin-2, and Dectin-3 are type II transmembrane receptors that contain a C-terminal carbohydrate recognition domain (CRD), a stalk region, a transmembrane domain, and an N-terminal cytoplasm tail (6, 12). Cytoplasmic tail of Dectin-1 has an ITAM for signaling transduction. In contrast, Dectin-2 and Dectin-3 contain only a short cytoplasmic domain and pair with the FcRγ chain to mediate signaling (20, 23–25). Ligation of these receptors induces Syk- and CARD9-dependent signaling cascades, leading to activation of the canonical NF-κB and expression of inflammatory cytokines such as TNF-α, IL-6, and IL-1β (20, 22, 25–29). Stimulation of these CLRs also induces several cellular events, including phagocytosis, neutrophil recruitment, inflammasome activation, and reactive oxygen species (ROS) production, which facilitate the clearance of fungi (13, 15, 17–20, 22–24, 27–33).

CD23, also named FcεRII or Clec4J, is another CLR and is expressed in mature B cells, eosinophils, monocytes, activated macrophages, follicular dendritic cells, and keratinocytes (34–37). Previous studies showed that CD23 mainly functions as a low-affinity receptor for IgE or as a B cell activation marker (38, 39). Moreover, it was reported that CD23 is involved in the clearance of *Mycobacterium avium* and *Leishmania* and *M. avium* infection by human macrophages (40, 41). Our recent study indicates that CD23 is significantly upregulated in the absence of JNK1 upon *C. albicans* infection, and this elevated CD23 plays important roles in JNK1-dependent negative regulation of antifungal immune responses (42). Structurally, CD23 is a typical type II CLR, which possesses CRD domain and intracellular ITAM-like motif. However, it remains to be determined whether CD23 functions as a PRR to sense microbial infection and to induce its downstream signaling.

In this study, we report that CD23 knockout (KO) mice are highly susceptible to infection with *C. albicans* and *A. fumigatus* but not with *C. neoformans*. Mechanistically, CD23 recognizes both α-mannan and β-glucan on *C. albicans* and *A. fumigatus* cell walls but does not recognize GXM from *Cryptococcus.* CD23 deficiency results in the impaired expression of NF-κB–dependent genes, especially inducible NO synthase (*iNOS*), which induces NO production to suppress infected fungi. Thus, our study reveals a CD23-induced antifungal signaling pathway and highlights the role of CD23 in antifungal effect for specific fungal species.

Materials and Methods

Mice

CD23 KO ($CD23^{-/-}$) mice were purchased from The Jackson Laboratory (stock no. 017795) and backcrossed with wild-type (WT) C57BL/6 mice for more than six generations. FcRγ KO mice were kindly provided by Prof. Fubin Li (Shanghai Jiao Tong University, Shanghai, China). To obtain $CD23^{-/-}$/$Rag1^{-/-}$ mice, $CD23^{-/-}$ mice were paired with $Rag1^{-/-}$ mice, and subsequent intercross of their offspring led to the generation of the double-KO mice. WT C57BL/6 mice were purchased from Vital River Laboratory Animal Technology (Beijing, China). All mice were housed in the specific pathogen-free animal facility at Tsinghua University. In all experiments described in this study, sex- and age-matched mice were used. All animal experiments were performed in compliance with institutional guidelines and according to the protocol approved by the Institutional Animal Care and Use Committee of Tsinghua University.

Abs and reagents

Abs against phosphorylated IκBα (9246), phosphorylated ERK (9101), phosphorylated JNK (9251), phosphorylated p38 (4631) and JNK (9252), p38 (9212), Dap12 (12492), SHP-1 (3759), SHP-2 (3397), and SHIP-1 (2726) were purchased from Cell Signaling Technology. Ab against FcRγ (06-727) was from Millipore; Abs against IκBα (sc-371), ERK (sc-154), β-tubulin (sc-8035), p65 (sc-8008), PCNA (sc-56), Rel-B (sc-226), and CD23 (sc-271900) were purchased from Santa Cruz Biotechnology. Abs against Flag (M20008) and HA (M20003) tag were from Abmart. Dectin-1 and Dectin-3 mAbs were generated by using the extracellular domain of Dectin-1 or Dectin-3 as immunogens, which was described before (20). PerCP/Cy5.5 anti-mouse CD45.2 (109827), FITC anti-mouse CD11b (101205), PE anti-mouse F4/80 (123109), Pacific Blue anti-mouse Gr-1 (108429), allophycocyanin anti-mouse CD11c (117309), PE anti-mouse CD23 (101608), and PE Rat IgG2a κ isotype control Abs (400507) were from BioLegend. PE anti-mouse CD86 (553692) Abs were from BD Pharmingen. Cy3-conjugated donkey anti-mouse IgG secondary Ab was purchased from Jackson ImmunoResearch (715-166-150). α-Mannan (M3640) was purchased from Sigma-Aldrich. Curdlan (030-09903) was obtained from Wako Chemicals. NF-κB inhibitor TPCA-1 (S2824) and NO donor molsidomine (S4664) were purchased from Selleck. CD23 blocking peptide (P30A, FHENWPS) and control peptide (SFNYNYA) were synthetized by GL Biochem (Shanghai, China). Clophosome clodronate liposomes or plain control liposomes were purchased from FormuMax Scientific. Mouse $CD11b^{+}$ cell depletion Ab (M1/70) was obtained from Bio X Cell.

Plasmids

Mouse CD23, Dectin-1, and Dectin-3 were amplified by PCR with cDNA of mouse bone marrow–derived macrophages (BMDMs) as template. PCR amplifying fragment was inserted into a lentivirus vector, p2K7, with the GatewayLR Clonase II Enzyme mix (11791020) from Invitrogen. Extracellular domains of CD23, Dectin-1, and Dectin-3 were amplified and inserted into pET28a vector between the EcoRI and XhoI sites. The PCR primers used were listed in Supplemental Table I.

Fungal strain

C. albicans strain 5314, *A. fumigatus* strain 293, *C. neoformans*–A strain H99, *C. gattii*–B strain WM179, and *C. neoformans*–AD strain WM628 were gifted from Prof. X. Jia (Tongji University, Shanghai, China).

Murine systemic fungal infection model

For in vivo *C. albicans* infection, mice were injected via lateral tail veins with 200 μl of a suspension containing different doses of *C. albicans* in sterile PBS (HyClone). For in vivo *A. fumigatus* and *C. neoformans* infection, mice were anesthetized by inhaling isoflurane and restrained on a small board, live fungi were inoculated in a 35-μl-volume sterile PBS into the trachea of each mouse. Mouse survival rates were monitored postinfection. Fungal loading was assessed by plating a series of diluted solutions of homogenized kidneys or lungs on yeast extract peptone dextrose or Sabouraud dextrose agar plates and culturing for 2 d, and the resulting colonies were counted. For cytokine measurement, extracts of kidney or lung tissue from infected mice were detected by Ready-SET-Go ELISA kits (eBioscience).

Ligand binding assay

Ligand binding assay was performed as previously described (20, 42). In brief, ELISA plates were coated with α-mannan, β-glucan, GXM-B, and GXM-D (40 μg/ml) overnight and then added with 100 μl/well renatured protein of recombinant protein at indicated concentrations. Bound proteins were detected by their respective mouse mAbs followed by HRP-conjugated goat anti-mouse IgG secondary Ab from EasyBio (BE0102). Tetramethylbenzidine substrate solution from eBioscience ELISA kit was used, and the reaction was stopped by 2 N H_2SO_4. OD 450 was read on a SpectraMax Plus 384 Microplate Reader.

Cellular binding assay

The cellular binding assay was performed as described with minor modification (15, 24). Briefly, RAW264.7 cells stably expressing Flag-tagged CD23, Dectin-1, or Dectin-3 were cocultured with GFP-labeled yeast (multiplicity of infection [MOI] = 5) or hyphae (MOI = 0.1) form of *C. albicans* for 10 min, and uncombined yeast (for yeast form binding) or Raw cells (for hyphae form binding) were removed by washing four times with medium. Then cells were fixed with 4% paraformaldehyde, permeabilized with 0.25% Triton X-100, and blocked with 10% goat serum. Anti-Flag from Abmart (M20008) was used as the first Ab, and Cy3-conjugated donkey anti-mouse IgG were used as the secondary Abs. DAPI (Beyotime Biotechnology) was counterstained to label the cell nuclear. Fluorescence was detected using a Zeiss LSM780 confocal laser scanning microscope.

BMDM preparation

Primary cultures of BMDMs from indicated mice were prepared as previously described (43). Briefly, bone marrow cells were harvested from the femurs and tibias of mice. Erythrocytes were removed from cells by using

a hypotonic solution. Cells were cultured for 7 d in DMEM containing 20% FBS, 55 μM 2-ME, streptomycin (100 μg/ml), penicillin (100 U/ml), and 30% conditioned medium from L929 cells expressing M-CSF. After 6–7 d of culturing, flow cytometry analysis indicated that the harvested cell population contained >97% $CD11b^+$, $F4/80^+$ cells.

Bone marrow–derived dendritic cell preparation

Primary cultures of bone marrow–derived dendritic cells from indicated mice were prepared as previously described (44). Briefly, bone marrow cells were harvested from the femurs and tibias of mice. Erythrocytes were removed from cells by using a hypotonic solution. Cells were cultured for 6–7 d in RPMI 1640 medium containing 20% FBS, 20 μg/ml GM-CSF, and 10 μg/ml IL-4. After 6–7 d of culturing, flow cytometry analysis indicated that the harvested cell population contained above 98% $CD11c^+$, MHC class II $(MHC\ II)^+$ cells.

Peritoneal macrophage preparation

Peritoneal macrophages (PMs) were prepared as previously described (43). Mice were i.p. injected with 2 ml of 4% thioglycolate, and 4 d later, PMs were isolated. Flow cytometry analysis indicated that the harvested cell population contained above 98% $CD11b^+$, $F4/80^+$ cells.

Immunoprecipitation and immunoblotting assay

For immunoblotting assay, cells were stimulated and lysed in lysis buffer (150 mM NaCl, 50 mM HEPES [pH 7.4], 1 mM EDTA, 1% Nonidet P-40, and protease inhibitors). Total cell lysates were then blotted using indicated Abs. For immunoprecipitation assay, cells were lysed in lysis buffer (250 mM NaCl, 50 mM HEPES [pH 7.4], 1 mM EDTA, 1% Nonidet P-40, 1 mM Na_3VO_4, 1 mM NaF, and 1 mM PMSF) supplemented with protease inhibitor. The immunoprecipitates and lysates were blotted using the indicated Abs.

Quantitative PCR

Total RNA was isolated using TRIzol (Invitrogen) and reverse transcribed using GoScript Reverse Transcriptase (Promega). Quantitative PCR was performed in triplicates using Power SYBR Green PCR Master Mix (Genestar). The amounts of transcript were normalized to GAPDH. Melting curves were run to ensure amplification of a single product. Primers used were listed in Supplemental Table I.

Cytokine measurement

Cytokine panels in the mouse kidney were detected with Ready-SET-Go ELISA kits (eBioscience) for TNF-α (88-7324-77), IL-1β (85-88-7013-88), IL-6 (88-7064-88), IL-12/IL-23 total p40 (85-88-7120-88), and IL-23 (85-88-7230-88). All samples were measured in triplicate according to the manufacturer's protocol.

Histopathology

For histopathology analyses, kidneys were fixed in 4% paraformaldehyde solution, embedded in paraffin, and sectioned. Five-micrometer-thick sections were stained with H&E, periodic acid–Schiff (PAS), Gomori methenamine silver (GMS), CD11b (GB11058), Ly-6G (GB11229), and F4/80 (GB11027), using standard staining procedures. Stained slides were scanned using a microscope (IX73; OLYMPUS).

FACS analysis

Kidney infiltrated immune cells and peripheral blood cells, including neutrophils, macrophages, and dendritic cells, were labeled with Abs specific for CD45.2, CD11b, F4/80, Gr-1, CD11c, and MHC II. Cells were analyzed by flow cytometry (BD LSRFortessa). Neutrophils were gated as $CD45.2^+$, $CD11b^+$, and $Gr\text{-}1^+$. Macrophages were gated as $CD45.2^+$, $CD11b^+$, and $F4/80^+$. Dendritic cells were gated as $CD45.2^+$, $CD11c^+$, and MHC II^+.

Macrophage and $CD11b^+$ cell depletion assay

For macrophage depletion, mice were i.p. injected with 200 μl of Clophosome clodronate liposomes or plain control liposomes (F70101C-N and F70101-N; FormuMax Scientific) 24 h before fungal infection. For $CD11b^+$ cell depletion, mice were i.p. injected with 100 μg M1/70 Ab 24 h before fungal infection. Forty-eight hours postinfection, mice were sacrificed and fungal loading was assessed by plating a series of diluted solutions of homogenized kidneys on the YPD plate.

NO concentration assay

Indicated cell culture supernatants were collected, and nitrite concentration was measured by a NO Assay Kit (catalog no. S0021; Beyotime) based on the Griess reaction. All samples were measured in triplicate according to the manufacturer's protocol.

Detection of ROS production

The production of ROS was assayed as described with minor modification (26). Briefly, 2×10^5 PMs were washed with PBS twice and resuspended in DMEM containing 10 μM DCFH-DA. Cells were incubated at 37°C for 30 min; after incubation, cells were washed with DMEM five times to remove the nonspecific binding. Then cells were infected with heat-killed *C .albicans* (HKC) at MOI = 10 for different time points, respectively. The relative number of ROS generated was detected every 10 min by flow cytometry measuring the mean fluorescence intensity.

Chromatin immunoprecipitation assay

The chromatin immunoprecipitation (ChIP) assay was performed with a ChIP kit (catalog no. 53009; Active Motif) as previously described (22, 42). The Abs used for ChIP are as follows: NF-κB p65 (sc-109) and Rel-B (sc-226). The resulting DNA was analyzed by real-time PCR. The PCR primers used were listed in Supplemental Table I.

Statistical analysis

All values in the paper are given as mean ± SEM unless stated otherwise. All in vitro experiments were reproduced at least three independent times, and all in vivo experiments were reproduced more than three times, unless stated otherwise. Statistical significance was calculated by two-tailed unpaired *t* test, multiple *t* test, or log-rank (Mantel–Cox) test using GraphPad Prism software. Statistical significance was set based on the *p* value: NS $p > 0.05$, $*p < 0.05$, $**p < 0.01$, and $***p < 0.001$.

Results

CD23 KO mice are susceptible to C. albicans *and* A. fumigatus *but not* C. neoformans *infection*

Our recent study suggests that CD23 may function to sense the surface components of *C. albicans* in antifungal immunity (42). However, it is not clear how CD23 functions as a fungal PRR and whether this effect is *C. albicans*–specific or not. To dissect the role of CD23 as a novel CLR and a PRR, we infected CD23 KO and their littermate CD23 heterozygous (CD23 Het) mice with different kinds of fungal species: *C. albicans*, *A. fumigatus*, *and C. neoformans*. Indeed, we found that CD23 KO mice had a lower survival rate than CD23 Het mice upon challenging with *C. albicans* and *A. fumigatus* but not *C. neoformans* (Fig. 1A–C), indicating that CD23 plays an important role in antifungal immune responses against *C. albicans* and *A. fumigatus*, but not *C. neoformans*, infection. Consistent with the lower survival rate, the fungal burden of *C. albicans* in kidneys and liver and *A. fumigatus* in lung postinfection was significantly higher in CD23 KO mice than in their heterozygous littermates (Fig. 1D, 1E, Supplemental Fig. 1A), but the burden of *C. neoformans*–A, *C. gattii*–B, and *C. neoformans*–AD in lungs were comparable in CD23 KO mice and CD23 Het mice (Fig. 1F).

Moreover, we examined the histopathology of the kidneys after *C. albicans* infection. CD23 KO mice showed severe kidney damage, as assessed by H&E and PAS staining. Fungal growth was detectable in the renal pelvis of CD23 KO mice with GMS staining, indicating that CD23 KO mice were unable to eradicate *C. albicans* (Fig. 1G). Because proinflammatory cytokines, such as TNF-α, IL-6, IL-23, and IL-1β, are indispensable for host antifungal immune responses (45, 46), we examined the expression level of proinflammatory cytokines in kidneys of mice infected with *C. albicans* and in lungs of *Cryptococcus*-infected mice and found that these cytokines in CD23 KO mice were significantly lower than those in CD23 Het mice after *C. albicans* infection (Fig. 1H) but found no difference after *Cryptococcus* infection (Fig. 1I). Together, these results demonstrated that CD23 is critical for the elimination of *C. albicans* and *A. fumigatus* infection but is not required for *Cryptococcus* clearance.

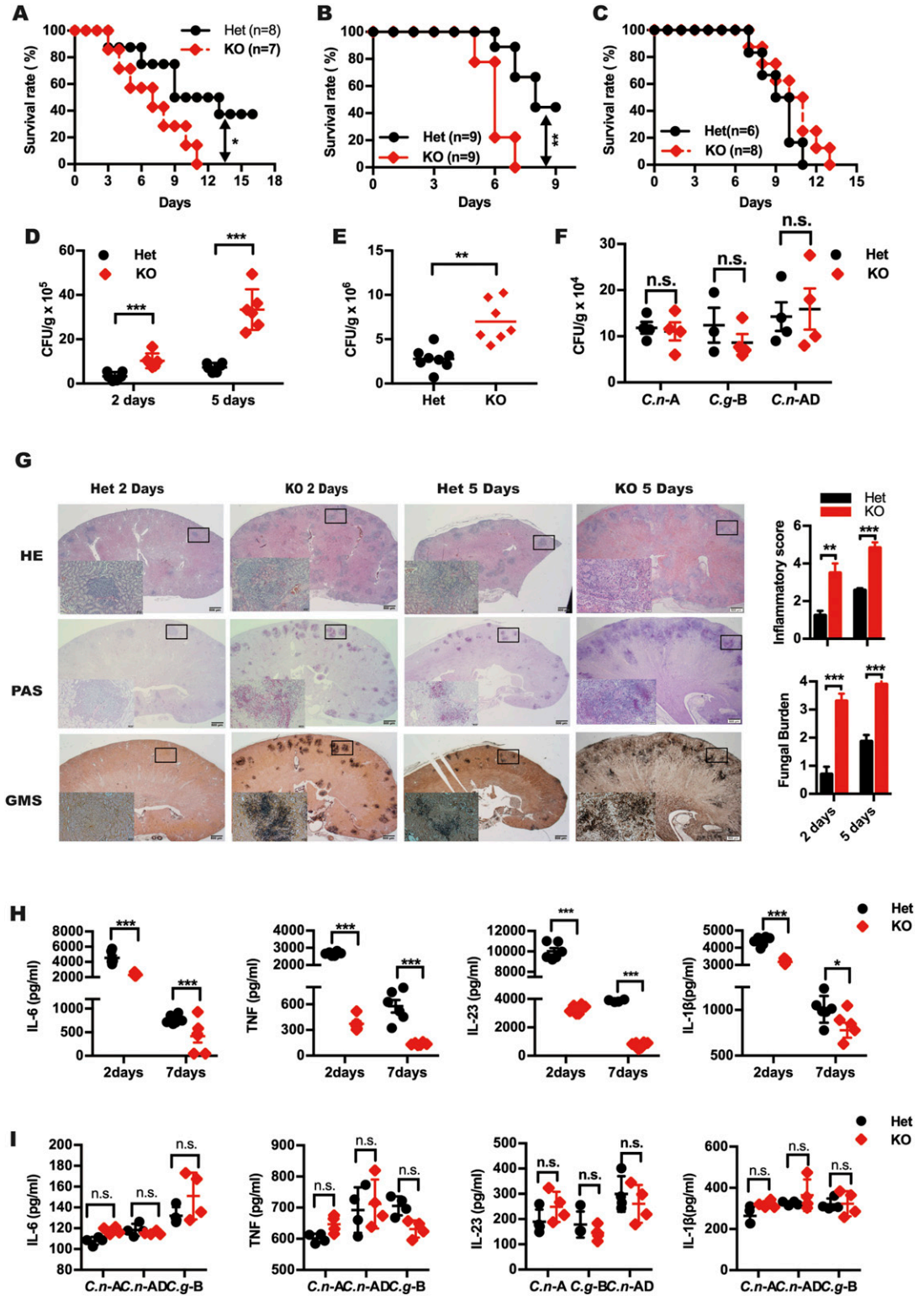

FIGURE 1. CD23 KO mice are susceptible to *C. albicans* and *A. fumigatus* but not *C. neoformans*. (**A**–**C**) Survival curves of WT, CD23 KO, and their littermate CD23 Het mice were i.v. injected with 5×10^5 CFU of *C. albicans* (strain 5314) (A) or 1×10^6 CFU of *A. fumigatus* (strain 293) (B) or given intratracheal infection with 1×10^5 CFU of *C. neoformans* serotype A (strain H99) (C). (**D**) CFU assays of kidneys of CD23 Het and CD23-deficient mice were i.v. injected with 5×10^5 CFU of *C. albicans* at day 2 and day 5 postinfection. (**E**) CFU assays of lungs of CD23 Het and CD23-deficient mice were intratracheally infected with 1×10^7 CFU of *A. fumigatus* at day 2 postinfection. (**F**) CFU assays of lungs of CD23 Het and CD23-deficient mice were intratracheally infected with 1×10^5 CFU of *C. neoformans* serotype A (strain H99), serotype B (strain WM179), and serotype AD (strain WM628) at day 3 postinfection. (**G**) Histopathology was analyzed with H&E, PAS, and GMS staining at day 2 and day 5 after i.v. injection with 5×10^5 CFU of *C. albicans*. Insets show regions of fungal inflammation and regions of fungal growth respectively. At least three mice were used, and three sections per kidney were analyzed. Insets show higher-magnification images of boxed areas. Scale bars, 500, 50 μm (insets). (**H**) Cytokines IL-6, TNF-α, IL-1β, and IL-23 of kidneys from CD23 Het and CD23-deficient mice i.v. injected with 5×10^5 CFU of *C. albicans* were assayed at day 2 and day 5 postinfection. (**I**) Cytokines IL-6, TNF-α, IL-1β, and IL-23 of kidneys from CD23 Het and CD23-deficient mice intratracheally infected with 1×10^5 CFU *(Figure legend continues)*

Macrophages are mainly responsible for the impaired antifungal immunity in CD23-deficient mice

CD23 is expressed in mature B cells, eosinophils, monocytes, activated macrophages, and follicular dendritic cells. To examine the impact by adaptive immune cells, we crossed CD23 KO mice with Rag1 KO mice to generate CD23/Rag1 double-KO mice. Although these mice lack T and B cells, CD23/Rag1 double-KO mice still showed a lower survival rate than CD23Het/Rag1 KO mice with *C. albicans* infection (Fig. 2A), indicating that CD23 expressed on non-T and B cells is responsible for the impaired antifungal immunity in CD23 KO mice.

It has been reported that macrophages and neutrophils are key effector cells for the host immune system to fight against fungi (45, 47). Macrophages constitute the first line of host defense against fungal infections, and the subsequent inflammatory response results in an influx of neutrophils and monocytes, leading to the second round of antifungal responses. To explore whether CD23 deficiency affects the immune cell infiltration after *C. albicans* infection, we determined cellular composition of kidneys and found that infected CD23 Het mice with *C. albicans* on day 2 showed a prominent infiltrating of $CD45.2^+$ immune cells, whereas CD23 deficiency significantly impaired $CD45.2^+$ immune cell accumulation in kidneys. On day 5 after *C. albicans* infection, CD23 KO mice accumulated more $CD45.2^+$ immune cells (Fig. 2B). Importantly, we found that fewer neutrophils were detected in kidneys of CD23 KO mice compared with heterozygous controls on day 2 postinfection, whereas there were only slightly fewer macrophages recruiting into kidneys in CD23 KO mice on day 2 postinfection (Fig. 2C, 2D). However, the infiltration of both neutrophils and macrophages in kidneys of CD23 KO mice was significantly increased at day 5 postinfection (Fig. 2C, 2D). The increased recruitment of inflammatory cells in the kidney of CD23 KO mice at this later infection time point is likely because the defected antifungal immunity in CD23 KO mice was unable to kill infected fungi at this time point, which results in recruiting more inflammatory cells.

To examine whether macrophages are responsible for the impaired antifungal immunity in CD23 deficiency mice, we depleted $CD11b^+$ cells by using M1/70 Ab and found that M1/70 Ab could deplete macrophages and neutrophils effectively (Fig. 2E–G). These mice were then infected with *C. albicans*, and fungal burden was analyzed. Although the fungal loading in kidneys of CD23 KO mice was significantly higher than that of WT mice, after depletion of macrophages, the fungal loading was comparable in kidneys of both CD23 Het and KO mice (Fig. 2H). To confirm this $CD11b^+$ Ab depletion experiment, we also used macrophage-depleting liposome and found that liposome-treated mice showed a performance similar to that of Ab-treated mice upon *C. albicans* infection (Fig. 2I). Moreover, macrophages from WT mice showed higher killing activities against *C. albicans* in vitro than those from CD23 KO mice (Fig. 2J) but showed comparable phagocytosis ability (Fig. 2K). However, there were no differences in killing activities and phagocytosis ability between neutrophils from CD23 Het and neutrophils from KO mice (Fig. 2L, 2M). Together, these data indicate that macrophages are mainly responsible for the impaired antifungal immunity in CD23-deficient mice.

CD23 recognizes surface components of C. albicans *and* A. fumigatus*, leading to NF-κB activation*

To determine whether CD23 directly recognizes fungal surface polysaccharide components, we examined the direct binding of recombinant protein containing the CD23 extracellular domain with plate-coated α-mannan and β-glucan, main components in cell walls of *C. albicans* and *A. fumigatus*, and GXMs extracted from *Cryptococcus* strains *C. gattii*–B and *C. neoformans*–AD. We found that CD23 protein could effectively bind with α-mannan and β-glucan, but not with GXMs (Fig. 3A), and the binding of CD23 to α-mannan and β-glucan was concentration dependent (Fig. 3B). Consistently, CD23 expressing on RAW264.7 cells were colocalized with yeast and hyphal forms of *C. albicans*, similar to Dectin-1 or Dectin-3 expressing on RAW264.7 cells (Fig. 3C). These results indicate that CD23 can directly bind to the surface components of *C. albicans* and *A. fumigatus*.

To determine the CD23 downstream signaling, we mutated the ITAM-like YSGY (CD23-WT) motif to FAGF (CD23-mutant [MUT]) in the intracellular domain of CD23 and expressed them in immortalized BMDM (iBMDM) cells. We found that cells expressing CD23-WT could effectively induce IκBα phosphorylation/degradation upon α-mannan stimulation, and this effect was abolished in cells expressing CD23-MUT, whereas NF-κB activation showed no differences between CD23-WT and CD23-MUT cells upon GXM stimulation (Fig. 3D). These results indicate that CD23 functions as a CLR recognizing α-mannan and β-glucan from *C. albicans* and *A. fumigatus*, but not GXMs from *C. neoformans*, to trigger NF-κB activation.

CD23 transduces proinflammatory signals in the FcRγ-dependent way

To further dissect the CD23 downstream signaling, an unbiased approach was designed to determine proteins interacting with the intracellular tail of CD23 (Fig. 4A). Lysates from BMDMs were incubated with biotinylated peptides corresponding to the intracellular domain of CD23 either unphosphorylated or phosphorylated at Tyr-6 and Tyr-9 residues (intracellular domain of phospho-Tyr). Biotinylated peptides were pulled down by using streptavidin beads, and the CD23-interacting proteins were analyzed by mass spectrometry. Top-ranked proteins specifically binding with CD23 were shown (Fig. 4B). Syk, Lyn, SHP-1, and SHP-2 were detected to bind with CD23 cytoplasmic tail. To confirm this mass spectrometry result, we performed the pull-down assay in BMDMs with the above CD23 peptides, and results confirmed the specific binding of FcRγ, Syk, SHP-1, and SHP-2 to unphosphorylated or phosphorylated CD23 peptides (Fig. 4C). Moreover, we performed the immunoprecipitation of CD23-WT or CD23-MUT from iBMDM cells ectopically expressing these proteins, and found that both CD23-WT and CD23-MUT could effectively associate with the endogenous FcRγ (Fig. 4D). However, this association was not dependent on ligand stimulation (Fig. 4D). To examine whether the association of CD23 with FcRγ depends on other protein(s), we coexpressed Flag-tagged CD23 and HA-tagged FcRγ in 293T cells and found that CD23 could associate with FcRγ with or without β-glucan stimulation (Fig. 4E), suggesting that CD23 may be directly associated FcRγ.

of *C. neoformans* serotype A, serotype B, and serotype AD at day 1 postinfection. Each dot represents a single mouse. Data are mean ± SEM (D–I). Statistical significance was calculated by log-rank (Mantel–Cox) test (A–C) and multiple *t* test (D–I). n.s. $p > 0.05$, $*p < 0.05$, $**p < 0.01$, $***p < 0.001$. n.s., not significant.

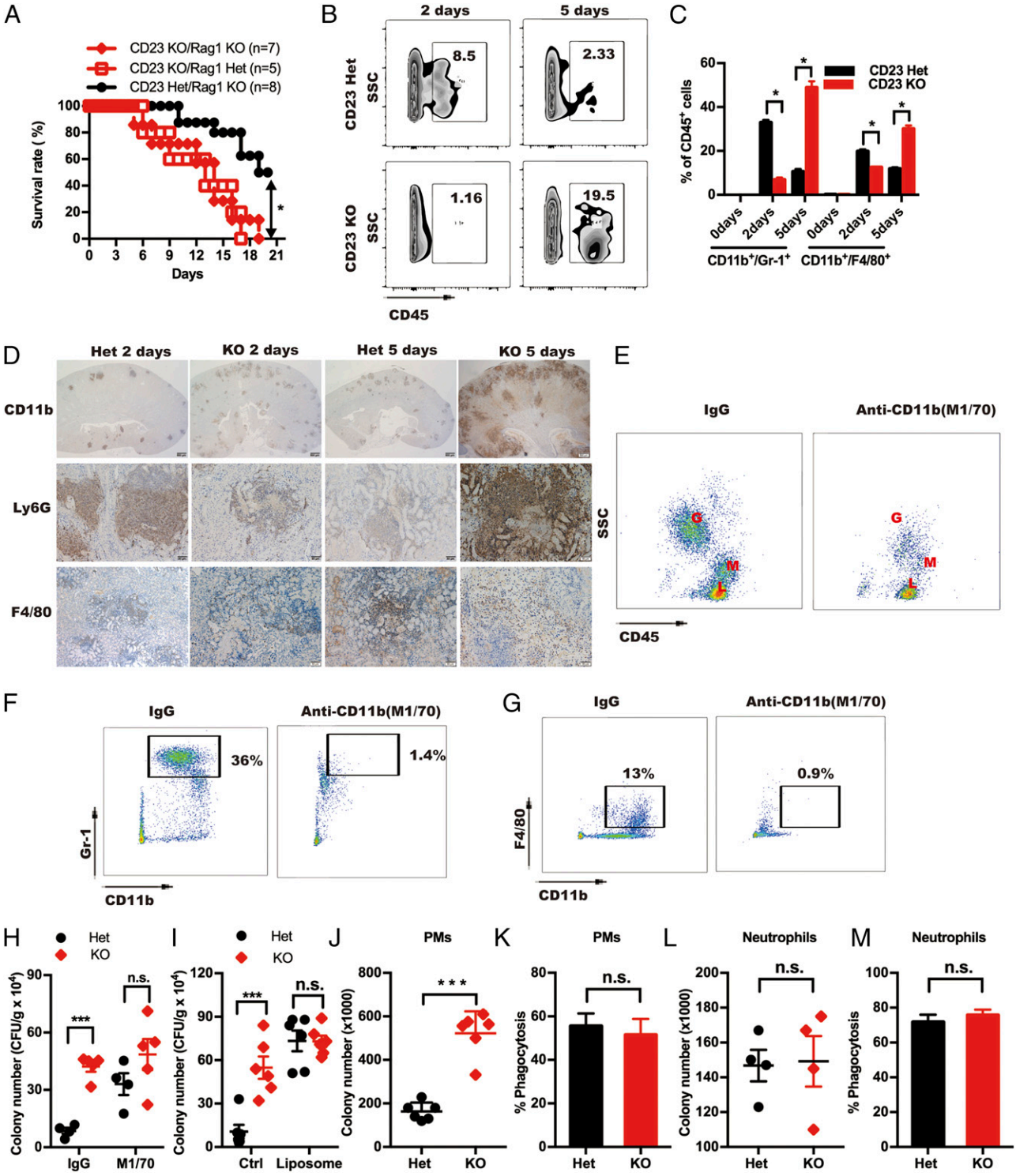

FIGURE 2. Macrophages are mainly responsible for the impaired antifungal immunity in CD23-deficient mice. (**A**) Survival curves of CD23 KO/Rag1 KO, CD23 KO/Rag1 Het, and CD23 Het/Rag1 KO mice were i.v. injected with 5×10^5 CFU of *C. albicans* (strain 5314). (**B**) FACS analysis of CD23 Het and KO mice kidneys infiltrating CD45.2$^+$ cells at day 2 and day 5 after i.v. injection with 5×10^5 CFU of *C. albicans*. (**C**) Statistical analysis of CD23 Het and KO mice kidneys infiltrating CD45.2$^+$/CD11b$^+$/Gr-1$^+$ neutrophils and CD45.2$^+$/CD11b$^+$/F4/80$^+$ macrophages at day 2 and day 5 after i.v. injection with 5×10^5 CFU of *C. albicans*. (**D**) Immunohistochemistry staining of CD11b$^+$, Ly-6G$^+$, and F4/80$^+$ cells of CD23 Het and KO mice kidneys at day 2 and day 5 after i.v. injection with 5×10^5 CFU of *C. albicans*. (**E**–**G**) FACS analysis of WT mice peripheral blood cell distribution after M1/70 and IgG treatment and at day 2 after 2×10^5 CFU of *C. albicans* infection; (E) FACS analysis of CD45.2$^+$ granular cell (G), monocyte and macrophage (M), and lymphocyte (L) distribution with M1/70 and IgG treatment; (F) FACS analysis of CD45.2$^+$/CD11b$^+$/Gr-1$^+$ neutrophils with M1/70 and IgG treatment; (G) FACS analysis of CD45.2$^+$/CD11b$^+$/F4/80$^+$ macrophages with M1/70 and IgG treatment. (**H**) CFU assays of kidneys of CD23 Het and CD23-deficient mice that were i.v. injected with 2×10^5 CFU of *C. albicans* at day 2 after IgG and M1/70 Ab treatment. (**I**) CFU assays of kidneys of CD23 Het and CD23-deficient mice that were i.v. injected with 2×10^5 CFU of *C. albicans* at day 2 after liposome treatment. (**J** and **K**) CD23 Het and KO PMs were isolated and cocultured with *C. albicans* (MOI = 5) for indicated time. (J) Killing ability was analyzed. (K) Phagocytosis ability was analyzed. (**L** and **M**) CD23 Het and KO neutrophils were isolated and cocultured with *C. albicans* (MOI = 5) for indicated time. (L) Killing ability was analyzed. (M) Phagocytosis ability was analyzed. Data are mean ± SEM (C and H–M). Data are representative of at least three independent experiments. Statistical significance was calculated by log-rank (Mantel–Cox) test (A) and multiple *t* test (C and H–M). n.s. $p > 0.05$, *$p < 0.05$, ***$p < 0.001$. n.s., not significant.

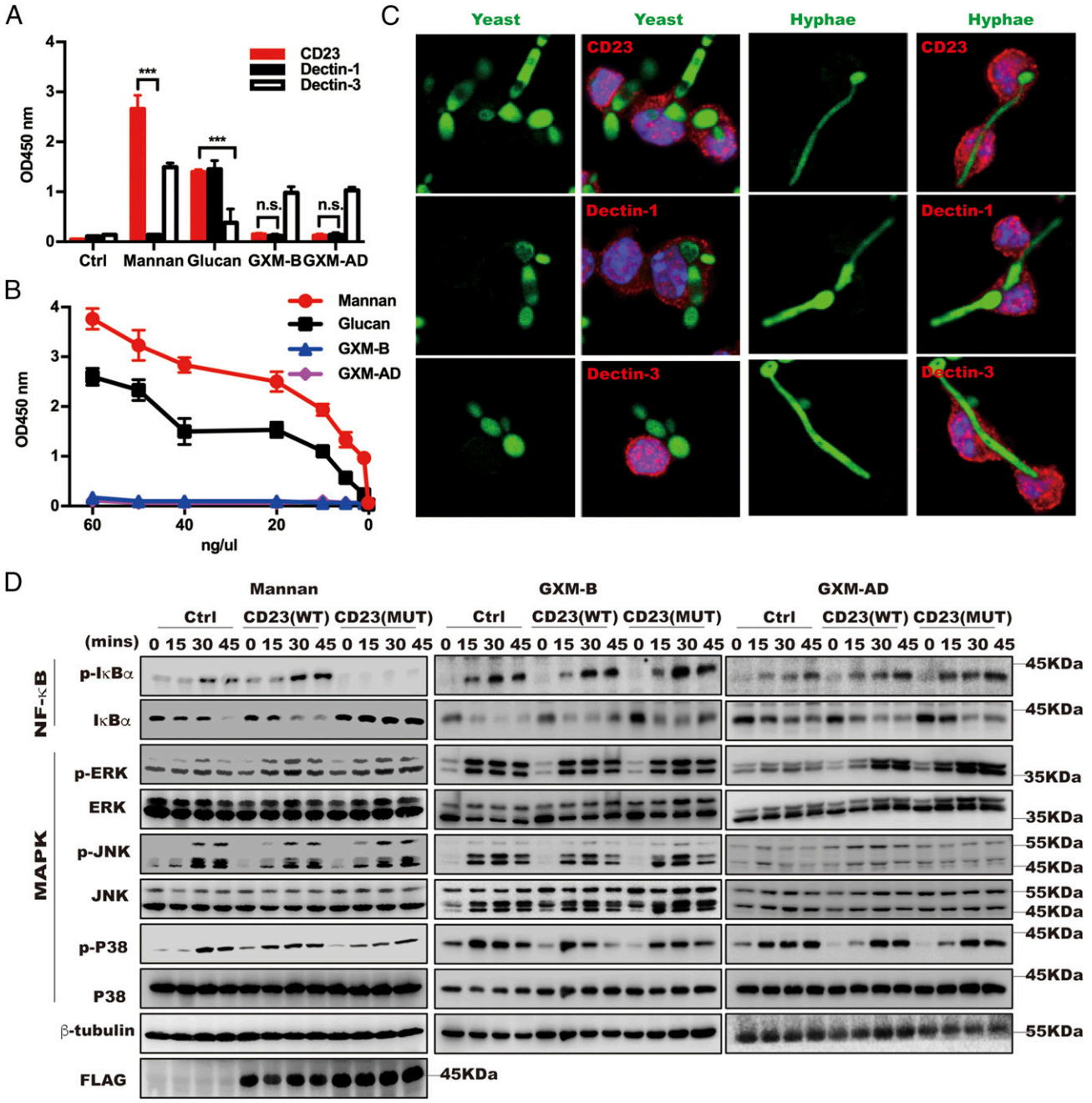

FIGURE 3. CD23 recognizes *C. albicans* and *A. fumigatus* surface components and leads to NF-κB activation. (**A** and **B**) Plates were precoated with 10 mg/ml (A) or different concentration (B) of α-mannan, β-glucan, GXM-B, and GXM-AD overnight. Renatured recombinant protein of CD23, Dectin-1, and Dectin-3 with indicated concentration was added and analyzed by ELISA. (**C**) RAW264.7 cells stably expressing Flag-tagged CD23, Dectin-1, or Dectin-3 were cocultured with UV cross-linked GFP-labeled yeast (MOI = 5) and hyphae (MOI = 0.1) form of *C. albicans* for 10 min and then stained with Flag-tagged CD23/Dectin-1/Dectin-3 (red). Cell nuclei were counterstained with DAPI (blue). Original magnification ×300. (**D**) iBMDM cells stably expressing Flag-tagged WT CD23, mutated CD23, or vector control were stimulated with precoated α-mannan (10 μg/ml), GXM-B (50 μg/ml), and GXM-AD (50 μg/ml) for the indicated time. Total cell lysates were analyzed by immunoblotting with Abs against total or phosphorylated IκBα, ERK, JNK, P38, or β-tubulin. Expression of Flag-tagged WT CD23 and mutated CD23 in transfected iBMDM cells was analyzed by immunoblotting with anti-Flag Ab. Data presented are from single experiments with at least three replica wells per condition. Data are mean ± SEM (A and B), and statistical significance was calculated by multiple *t* test (A and B). ***$p < 0.001$.

Previous studies showed that P30A could downregulate CD23 level in B cells and inhibit the production of CD23-dependent inflammatory mediators in monocytes and macrophages (48), and our recent studies found that P30A could efficiently trigger CD23 endocytosis in macrophages (42). Therefore, we isolated PMs from WT or FcRγ KO mice and stimulated cells in the presence or absence of P30A peptide. We found that blocking of CD23 by P30A in WT macrophage indeed decreased the expression of TNF-α and IL-6 to the level of FcRγ KO macrophages. However, FcRγ KO cells expressed similar amounts of TNF-α and IL-6 with or without the CD23-blocking peptide (Fig. 4F), suggesting that CD23 transduces proinflammatory signals in the FcRγ-dependent manner.

CD23 is necessary for C. albicans*–induced NF-κB activation in activated macrophages*

To determine how macrophage-expressed CD23 influences antifungal immune responses, BMDMs were isolated from CD23 Het and KO mice and stimulated with *C. albicans*. Surprisingly,

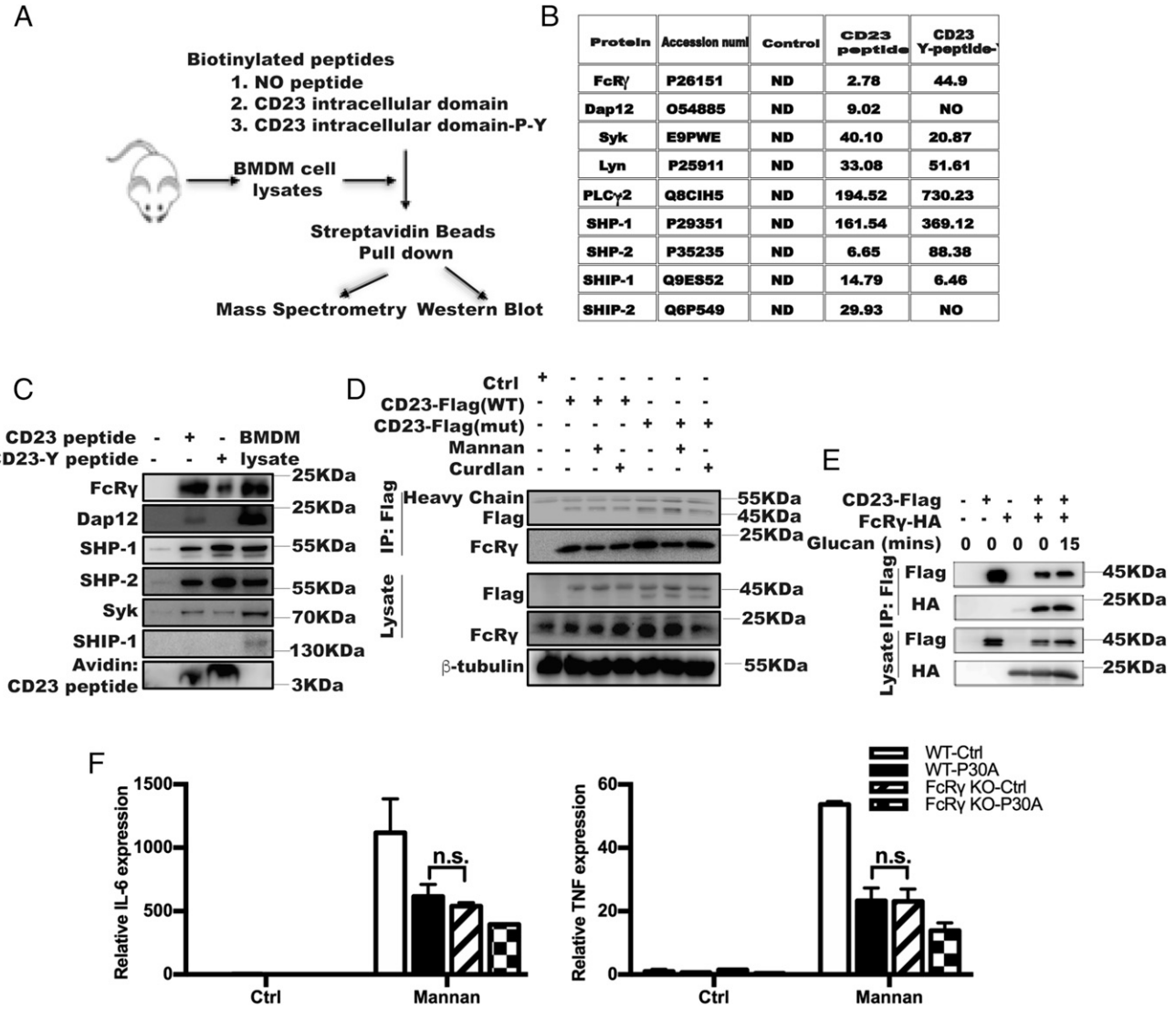

FIGURE 4. CD23 transduces proinflammatory signals in the FcRγ-dependent manner. (**A**–**C**) Lysates from BMDMs were incubated with peptides representing the intracellular domain of CD23 or Y6 and Y9 doubly-phosphorylated CD23 (CD23-P). Incubation without peptide was used as a negative control. Pull-down of these peptides was then performed with streptavidin-conjugated beads, and interacting proteins were analyzed by mass spectrometry or Western blot. (A) Workflow is shown. (B) Unique peptide counts determined by mass spectrometry from selected proteins, with their accession numbers. (C) Western blot of selected proteins pulled down in the assay. A representative blot of three performed is shown. (**D**) iBMDM cells stably expressing Flag-tagged WT CD23, mutated CD23, or mock vector were lysed. Cell lysates were immunoprecipitated with Flag Ab, and then the immunoprecipitated (IP) and lysate fractions were analyzed by immunoblotting with the indicated Abs. (**E**) HEK293T cells were transfected with Flag-tagged CD23 together with HA-tagged FcRγ with β-glucan (50 μg/ml) stimulation for the indicated time and then lysed. Cell lysates were immunoprecipitated with Flag Ab, and then the immunoprecipitated (IP) and lysate fractions were analyzed by immunoblotting with the indicated Abs. (**F**) WT and FcRγ-deficient thioglycolate-elicited PMs were stimulated with precoated α-mannan (10 μg/ml). CD23 blocking P30A peptide or control peptide were added when cells were added to the coated plate. Six hours later, supernatant was collected and ELISA assay was performed to detect the production of TNF-α and IL-6. Data are representative of at least three independent experiments. Data are mean ± SEM (F), and statistical significance was calculated by multiple *t* test (F). ND, not detected; n.s., $p > 0.05$, not significant.

we found that there was no significant difference of IκBα phosphorylation/degradation and MAPK activation (p38, ERK, and JNK) between CD23 Het and CD23 KO BMDMs after *C. albicans* stimulation (Supplemental Fig. 1B). Inflammatory cytokine production also showed no significant difference between CD23 KO and control groups (Supplemental Fig. 1C). Because our recent work showed that CD23 was upregulated 24 h after fungal infection (42), it suggests that CD23 may mainly express and function in activated macrophages. It has been shown that murine CD23 has three dominant splicing isoforms, which resulted from the alternative transcription initiation. These isoforms display a cell-specific expression pattern and differ only by the first N-terminal amino acids of the intracellular region (49–52). We examined the expression level of different CD23 isoforms in BMDMs upon *C. albicans* stimulation and found that the isoform with amino acids MEENEYS in its first exon was predominantly expressed (Supplemental Fig. 1D). Because PMs have been reported to be activated macrophages (43, 53), we examined the surface activation markers and CD23 expression in PMs and BMDMs. We found that PMs expressed higher levels of CD86 (M1 phase macrophage marker) and CD23 (Supplemental Fig. 1E); we also examined the relative expression of CD23 in iBMDMs, BMDMs with or without *C. albicans* stimulation together with PMs, and found that the expression of CD23 was

higher in *C. albicans*–stimulated iBMDMs and PMs (Supplemental Fig. 1F), indicating that CD23 is expressed in more activated macrophages, such as PMs. Therefore, we examined the downstream signaling event of CD23 by using PMs from CD23 Het and KO mice. Significantly decreased IκBα phosphorylation was observed in CD23 KO cells compared with control cells upon the stimulation by α-mannan and β-glucan (curdlan), but MAPK activation was comparable between CD23 Het and KO cells (Fig. 5A). However, there were no differences between cells from CD23 Het and KO mice with GXM stimulation (Fig. 5B).

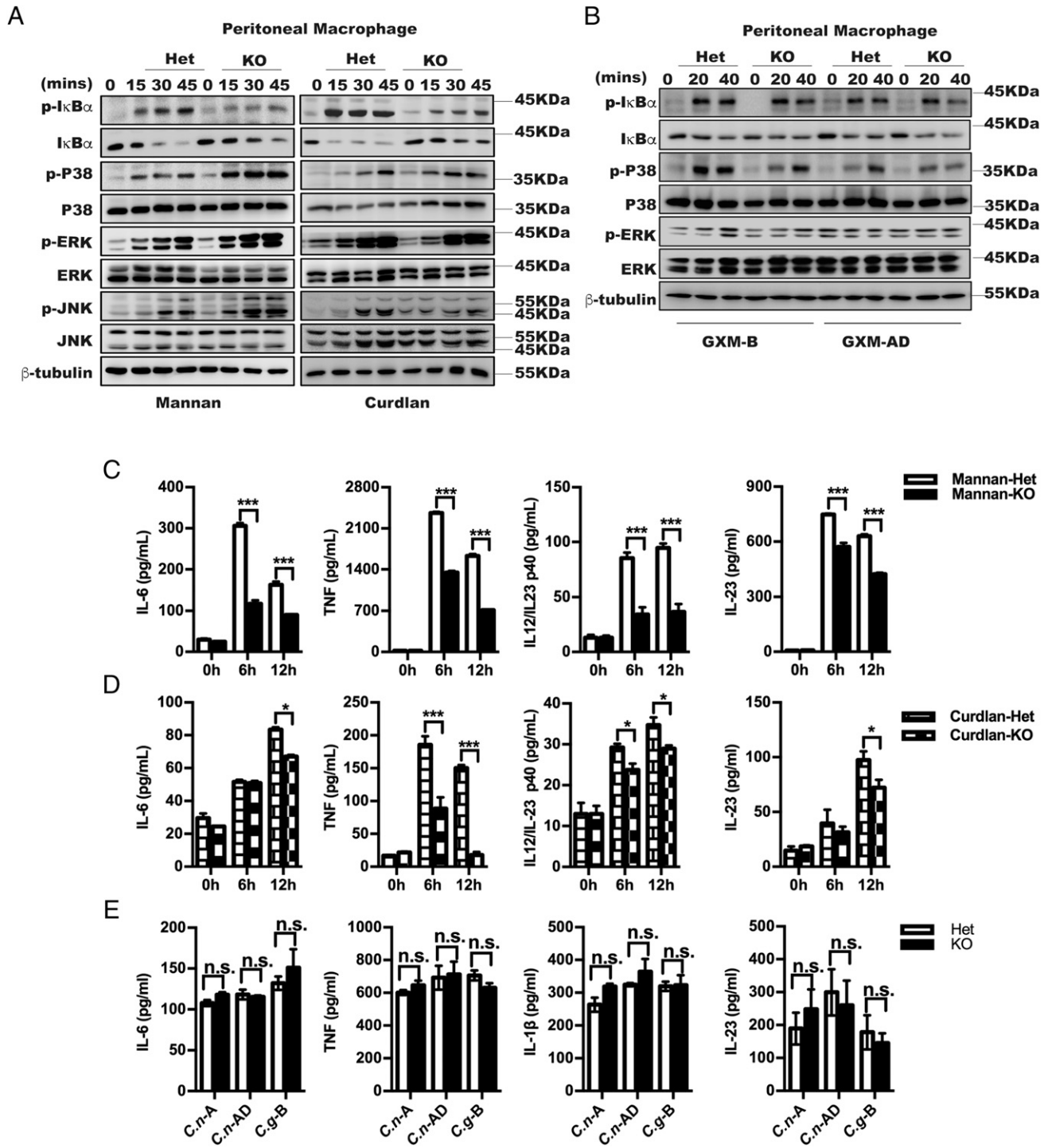

FIGURE 5. CD23 is required for *C. albicans*–induced NF-κB activation and inflammatory responses in activated macrophages. (**A** and **B**) CD23 Het and KO mice PMs were stimulated with 10 μg/ml precoated α-mannan, 50 μg/ml precoated curdlan (A), GXM-B, or GXM-AD (B) for indicated time and then lysed. Total cell lysates were analyzed by immunoblotting with Abs against total or phosphorylated IκBα, ERK, P38, JNK, or β-tubulin. (**C** and **D**) CD23 Het and KO PMs were stimulated with 10 μg/ml precoated α-mannan (C) and 50 μg/ml precoated curdlan (D) for 6 and 12 h, and proinflammatory cytokine IL-6, TNF-α, IL-23, and IL-1β expression was analyzed by ELISA. (**E**) CD23 Het and KO PMs were stimulated with *C. neoformans*–A, *C. gattii*–B, and *C. neoformans*–AD (MOI = 5) for 12 h, and proinflammatory cytokine IL-6, TNF-α, IL-23, and IL-1β expression was analyzed by ELISA. Data are representative of at least three independent experiments. Statistical significance was calculated by multiple *t* test (C–E). Data are mean ± SEM (C–E). n.s. $p > 0.05$, *$p < 0.05$, ***$p < 0.001$. n.s., not significant.

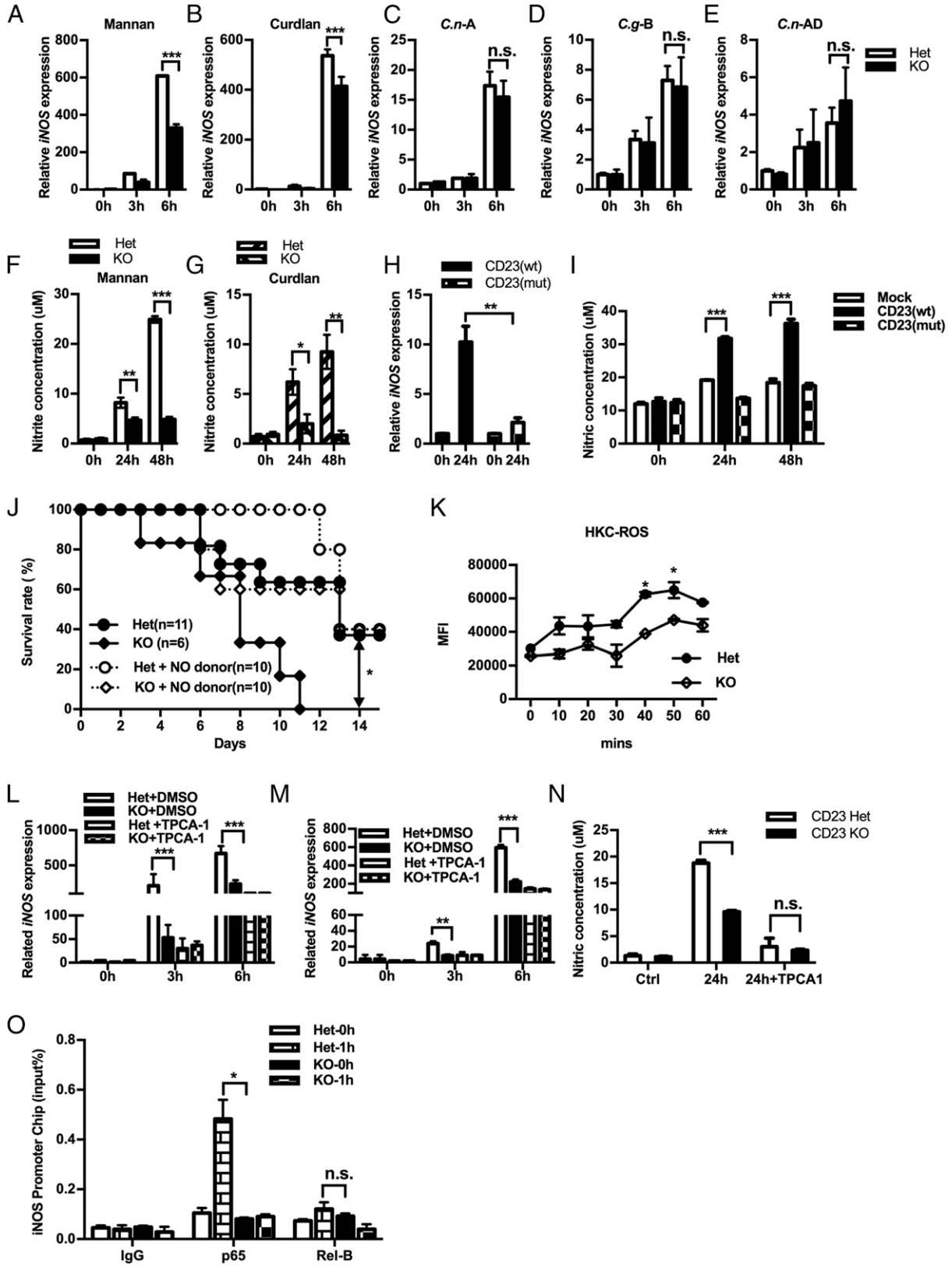

FIGURE 6. CD23 regulates iNOS expression through NF-κB activation, and NO is indispensable for antifungal immune response. (**A** and **B**) CD23 Het and KO PMs were stimulated with 10 μg/ml precoated α-mannan (A) and 50 μg/ml precoated curdlan (B) for indicated time; mRNA was collected, and *iNOS* expression was analyzed by RT-PCR. (**C**–**E**) CD23 Het and KO PMs were stimulated with *C. neoformans*–A, *C. gattii*–B, and *C. neoformans*–AD (MOI = 5) for indicated time; mRNA was collected, and *iNOS* expression was analyzed by RT-PCR. (**F** and **G**) CD23 Het and KO PMs were stimulated with 10 μg/ml precoated α-mannan (F) and 50 μg/ml precoated curdlan (G) for indicated time; NO production in culture supernatants was measured by nitrite assay kit. (**H** and **I**) iBMDM cells stably expressing Flag-tagged WT CD23, mutated CD23, or vector control were stimulated with 10 μg/ml precoated α-mannan or HKC (MOI = 5) for the indicated time. (H) *iNOS* mRNA levels were measured by RT-PCR. (I) NO production in culture supernatants was measured by nitrite assay kit. (**J**) Survival curves of CD23 Het and KO mice ($n > 6$ for each group) were i.v. injected with *(Figure legend continues)*

Moreover, the secretion of proinflammatory cytokines (IL-6, TNF-α, IL-12, and IL-23) was impaired in CD23 KO PMs upon α-mannan and β-glucan (curdlan) stimulation (Fig. 5C, 5D), but there were no differences between CD23 Het and KO PMs with *Cryptococcus* stimulation (Fig. 5E). Dendritic cells are also key effector cells for the host immune system to fight against fungi, and we also detected IκBα phosphorylation and degradation in bone marrow–derived dendritic cells from CD23 Het and KO mice. However, there were no differences between cells from CD23 Het and KO mice with either α-mannan or β-glucan (curdlan) stimulation (Supplemental Fig. 2A); the production of inflammatory cytokines also showed no significant difference (Supplemental Fig. 2B). Together, these data suggest that CD23 mainly expresses in activated macrophages, recognizing α-mannan and β-glucan from *C. albicans* and *A. fumigatus*, but not GXMs from *C. gattii*–B and *C. neoformans*–AD, to trigger NF-κB–mediated proinflammation responses.

CD23 regulates iNOS expression through NF-κB, and NO is indispensable for the antifungal immune response

The major gene expressed by activated M1 macrophage is *iNOS*, and NO is able to kill different infected microbial organisms including fungi (40, 42, 54). Our previous paper also showed that elevated NO production in JNK1 KO cells or mice contributes to the enhanced antifungal effect (42). Interestingly, we found that CD23 KO PMs stimulated with α-mannan or curdlan (Fig. 6A, 6B), but not *C. neoformans*–A, *C. gattii*–B, and *C. neoformans*–AD (Fig. 6C–E), expressed fewer *iNOS* mRNA than CD23 Het cells, and less NO was detected in the supernatant of CD23 KO cells (Fig. 6F, 6G). Consistently, α-mannan stimulation could upregulate *iNOS* expression and NO production in cells expressing CD23-WT but not CD23-MUT (Fig. 6H, 6I). To determine whether defective NO production is responsible for the impaired antifungal immunity in CD23 KO mice, we treated CD23 KO and control mice with NO donor (molsidomine) or vehicle control. We found that NO donor indeed could rescue the impaired antifungal immunity in CD23 KO mice (Fig. 6J). ROS production has been reported to be important for the antifungal response (26, 55, 56), and NO can interact with ROS to form peroxynitrite and can efficiently kill fungi (45, 57). We found that CD23 KO cells produced fewer ROS upon fungal stimulation (Fig. 6K).

Next, we examined how CD23 regulates *iNOS* expression and NO production. Previous papers have reported that ERK, P38, JNK, NF-κB, IRF-1, and STAT1 can induce NO secretion (58–61). Because CD23 can regulate NF-κB activation, we examined whether iNOS induction is through a NF-κB–dependent mechanism. IKK inhibitor TPCA-1 was used to inhibit NF-κB activation, and we then examined *iNOS* expression following the stimulation by α-mannan, curdlan, or HKC. Indeed, we found that *iNOS* expression and NO production were significantly reduced upon TPCA-1 treatment (Fig. 6L–N), indicating that CD23 regulates *iNOS* expression and NO production in a NF-κB–dependent manner. Because two putative NF-κB binding sites (−971 to −962: 5′-GGGATTTTCC-3′ and −85 to −76: 5′-GGGACTCTCC-3′) were found in *iNOS* promoter region, we performed ChIP assay and found that there was strong binding of NF-κB to *iNOS* promoter at −971 to −962 site following *C. albicans* stimulation (Fig. 6O). Together, these data indicate that CD23 regulates *iNOS* expression through transcription factor NF-κB directly binding to *iNOS* promoter (Fig. 7), and *iNOS*-produced NO plays an important role in antifungal immunity.

Discussion

In this study, we characterized the function of a novel CLR, CD23, in the antifungal immune responses and elucidated its downstream signaling events. We found that CD23 KO mice are susceptible to *C. albicans* and *A. fumigatus* but not *C. neoformans*. Macrophages are mainly responsible for the impaired antifungal immunity in CD23-deficient mice, and CD23 could directly recognize α-mannan and β-glucan from *C. albicans* and *A. fumigatus*, but not GXMs from *C. neoformans*, in a FcRγ-dependent way. Moreover, CD23 regulates iNOS expression and NO production through NF-κB activation for antifungal immune response (Fig. 7).

CLRs initiate the antifungal immune response. It has been reported that Dectin-1 (15, 62–64), Dectin-2 (18, 24, 28), Dectin-3 (20, 65), Mincle (34, 66), mannose receptor (MR) (67, 68), DC-SIGN (69, 70), SIGNR1 (71), and Galectin-3 (72) can sense fungal infection by recognizing different components of the cell wall of *C. albicans*, *A. fumigatus*, and *C. neoformans*. However, it remains to be determined whether other CLRs are involved in the host antifungal response. In our current and previous study (42), we have provided strong evidence indicating that CD23 functions as a CLR to sense fungal infection. It remains to address whether other uncharacterized CLRs are also involved in regulation of the host antifungal immune response.

Neutrophil recruitment at the initial stage upon fungal infection is a key event to eradicate fungi. Several groups have shown that fungal-sensed monocytes, especially macrophages, secrete cytokines and chemokines to recruit and activate neutrophils (73, 74), and recruited neutrophils can induce phagocytosis or produce toxic agents, including ROS, to eradicate fungi (75). In the first 2 d postinfection, neutrophils and inflammatory monocytes accumulate in almost equal amounts in kidneys. However, the influx of inflammatory monocytes was transient, peaking at day 1 and declining thereafter. In contrast, neutrophils display a second wave of massive infiltration starting between day 3 and day 5 postinfection (73, 74, 76). Our studies find that fewer neutrophils and macrophages are detected in CD23 KO mice at day 2, whereas both of them were spread at day 5; this continuous recruitment of neutrophils is likely an overreactive host response against the higher fungal burden in CD23 KO mice. Interestingly, activated macrophages dominate antifungal immunity. Therefore, macrophage

5×10^5 CFU of *C. albicans* (5314); mice were gavaged with NO donor (molsidomine, 10 mg/kg) or vehicle control every 2 d. (**K**) CD23 Het and KO PMs were stimulated with HKC (MOI = 5), and cells were labeled with DCFH-DA probe, and relative number of ROS generated was detected every 10 min by flow cytometry measuring the mean fluorescence intensity. (**L–N**) CD23 Het and KO PMs were stimulated with 10 μg/ml precoated α-mannan (L), 50 μg/ml precoated curdlan (M), or HKC (MOI = 5) (N), and 1 μM TPCA-1 (NF-κB inhibitor) was added to cells when stimulation began; after stimulation for indicated time, mRNA was collected and *iNOS* expression was analyzed by RT-PCR (L and M). NO production in culture supernatants was measured by nitrite assay kit (N). (**O**) CD23 Het and KO PMs were stimulated with 10 μg/ml precoated α-mannan for 1 h, and resulting cells were subjected to ChIP assays with the indicated Abs, followed by RT-PCR analysis for the *iNOS* promoter. Data are representative of at least three independent experiments. Data are mean ± SEM (A–I and K–O), and statistical significance was calculated by log-rank (Mantel–Cox) test (J) and multiple *t* test (A–I and K–O). n.s. $p > 0.05$, *$p < 0.05$, **$p < 0.01$, ***$p < 0.001$. n.s., not significant.

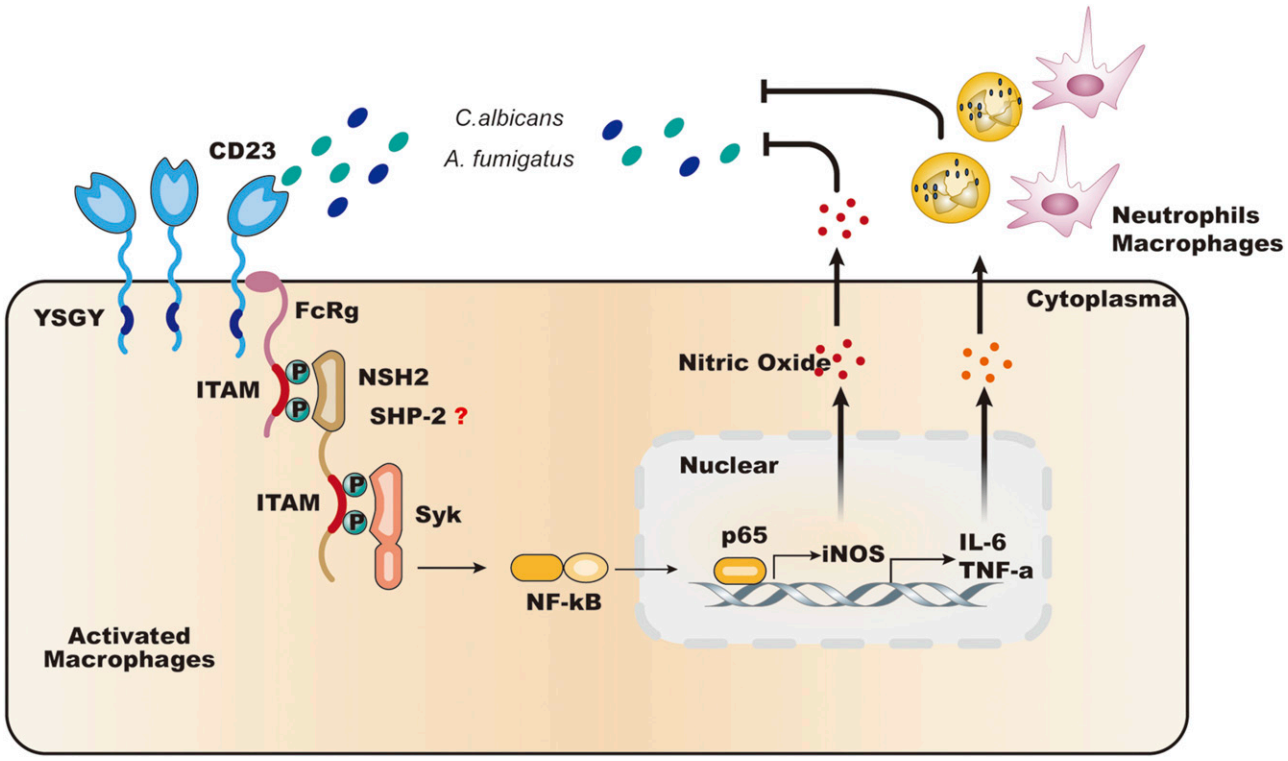

FIGURE 7. Proposed model for the mechanism by which CD23 regulates antifungal immune response. In the activated macrophage, *C. albicans and A. fumigatus* are sensed by CLR CD23; after ligation of CD23 by *C. albicans* and *A. fumigatus* α-mannan and β-glucan, CD23 recruit adaptor protein FcRγ to trigger NF-κB activation, and NF-κB regulated proinflammatory cytokine production, which is critical for recruiting of neutrophils and monocytes helping host clearance of fungi. Moreover, NF-κB p65 subunit will transport to the nucleus and bind with *iNOS* promoter to induce higher *iNOS* expression, and these lead to higher level of NO production to kill *C. albicans* and *A. fumigatus*.

depletion in WT mice resembles the phenotype similar to CD23 KO mice.

The role of NO in clearing pathogen infection has been documented. Activated macrophages are the main source of NO production, controlled by the catalytic action of iNOS in response pathogen infection. NO has been shown to contribute to the host defense against *Toxoplasma gondii*, *Leishmania major* (77), and *M. tuberculosis* (58, 78). SCID mice are more susceptible to mucosal *Candida* infections upon iNOS inhibition, and macrophages from these mice showed reduced candidacidal activity upon iNOS inhibitor treatment in vitro (79). However, it was reported that inhibitors of NO production did not inhibit killing of *Candida* by human dendritic cells (80). In this study, we show that deficiency of NO production is definitely the reason for the impaired antifungal immunity in CD23 KO mice because NO donors can rescue the phenotype. CD23 controls NO production through NF-κB p65 subunit by binding to *iNOS* promoter. Additionally, NO may interact with ROS to form peroxynitrite to efficiently kill fungi as previously reported (45, 57).

In summary, we show CD23 functions as a CLR to initiate the host antifungal response against *C. albicans* and *A. fumigatus* infection but not *C. neoformans* infection. This function of CD23 is through its downstream signaling cascade, leading to induction of NF-κB–dependent iNOS expression and ultimately to NO production by activated macrophages. Therefore, our study provides the molecular insight for developing novel approaches to fight fungal infection.

Acknowledgments

We thank Dr. Fubin Li for providing the FcRγ KO mice. We thank Libing Mu for drafting the proposed model.

Disclosures

The authors have no financial conflicts of interest.

References

1. Brown, G. D., D. W. Denning, N. A. Gow, S. M. Levitz, M. G. Netea, and T. C. White. 2012. Hidden killers: human fungal infections. *Sci. Transl. Med.* 4: 165rv13.
2. Brown, G. D., D. W. Denning, and S. M. Levitz. 2012. Tackling human fungal infections. *Science* 336: 647.
3. Netea, M. G., L. A. Joosten, J. W. van der Meer, B. J. Kullberg, and F. L. van de Veerdonk. 2015. Immune defence against candida fungal infections. *Nat. Rev. Immunol.* 15: 630–642.
4. LeibundGut-Landmann, S., M. Wüthrich, and T. M. Hohl. 2012. Immunity to fungi. *Curr. Opin. Immunol.* 24: 449–458.
5. Idnurm, A., Y. S. Bahn, K. Nielsen, X. Lin, J. A. Fraser, and J. Heitman. 2005. Deciphering the model pathogenic fungus *Cryptococcus neoformans*. *Nat. Rev. Microbiol.* 3: 753–764.
6. Netea, M. G., G. D. Brown, B. J. Kullberg, and N. A. Gow. 2008. An integrated model of the recognition of *Candida albicans* by the innate immune system. *Nat. Rev. Microbiol.* 6: 67–78.
7. Plato, A., S. E. Hardison, and G. D. Brown. 2015. Pattern recognition receptors in antifungal immunity. *Semin. Immunopathol.* 37: 97–106.
8. Gastebois, A., C. Clavaud, V. Aimanianda, and J. P. Latgé. 2009. *Aspergillus fumigatus*: cell wall polysaccharides, their biosynthesis and organization. *Future Microbiol.* 4: 583–595.
9. Dromer, F., E. Gueho, O. Ronin, and B. Dupont. 1993. Serotyping of *Cryptococcus neoformans* by using a monoclonal antibody specific for capsular polysaccharide. *J. Clin. Microbiol.* 31: 359–363.
10. Zaragoza, O., M. L. Rodrigues, M. De Jesus, S. Frases, E. Dadachova, and A. Casadevall. 2009. The capsule of the fungal pathogen *Cryptococcus neoformans*. *Adv. Appl. Microbiol.* 68: 133–216.
11. Gauglitz, G. G., H. Callenberg, G. Weindl, and H. C. Korting. 2012. Host defence against *Candida albicans* and the role of pattern-recognition receptors. *Acta Derm. Venereol.* 92: 291–298.
12. Hardison, S. E., and G. D. Brown. 2012. C-type lectin receptors orchestrate antifungal immunity. *Nat. Immunol.* 13: 817–822.
13. Vautier, S., D. M. MacCallum, and G. D. Brown. 2012. C-type lectin receptors and cytokines in fungal immunity. *Cytokine* 58: 89–99.
14. Steele, C., R. R. Rapaka, A. Metz, S. M. Pop, D. L. Williams, S. Gordon, J. K. Kolls, and G. D. Brown. 2005. The beta-glucan receptor dectin-1 recognizes specific morphologies of *Aspergillus fumigatus*. *PLoS Pathog.* 1: e42.

15. Taylor, P. R., S. V. Tsoni, J. A. Willment, K. M. Dennehy, M. Rosas, H. Findon, K. Haynes, C. Steele, M. Botto, S. Gordon, and G. D. Brown. 2007. Dectin-1 is required for beta-glucan recognition and control of fungal infection. *Nat. Immunol.* 8: 31–38.
16. Nakamura, K., T. Kinjo, S. Saijo, A. Miyazato, Y. Adachi, N. Ohno, J. Fujita, M. Kaku, Y. Iwakura, and K. Kawakami. 2007. Dectin-1 is not required for the host defense to *Cryptococcus neoformans*. *Microbiol. Immunol.* 51: 1115–1119.
17. McGreal, E. P., M. Rosas, G. D. Brown, S. Zamze, S. Y. Wong, S. Gordon, L. Martinez-Pomares, and P. R. Taylor. 2006. The carbohydrate-recognition domain of Dectin-2 is a C-type lectin with specificity for high mannose. *Glycobiology* 16: 422–430.
18. Saijo, S., S. Ikeda, K. Yamabe, S. Kakuta, H. Ishigame, A. Akitsu, N. Fujikado, T. Kusaka, S. Kubo, S. H. Chung, et al. 2010. Dectin-2 recognition of alpha-mannans and induction of Th17 cell differentiation is essential for host defense against *Candida albicans*. *Immunity* 32: 681–691.
19. Yonekawa, A., S. Saijo, Y. Hoshino, Y. Miyake, E. Ishikawa, M. Suzukawa, H. Inoue, M. Tanaka, M. Yoneyama, M. Oh-Hora, et al. 2014. Dectin-2 is a direct receptor for mannose-capped lipoarabinomannan of mycobacteria. *Immunity* 41: 402–413.
20. Zhu, L. L., X. Q. Zhao, C. Jiang, Y. You, X. P. Chen, Y. Y. Jiang, X. M. Jia, and X. Lin. 2013. C-type lectin receptors Dectin-3 and Dectin-2 form a hetero-dimeric pattern-recognition receptor for host defense against fungal infection. *Immunity* 39: 324–334.
21. Hole, C. R., C. M. Leopold Wager, A. S. Mendiola, K. L. Wozniak, A. Campuzano, X. Lin, and F. L. Wormley, Jr. 2016. Antifungal activity of plasmacytoid dendritic cells against *Cryptococcus neoformans* in vitro requires expression of Dectin-3 (CLEC4D) and reactive oxygen species. *Infect. Immun.* 84: 2493–2504.
22. Zhao, X. Q., L. L. Zhu, Q. Chang, C. Jiang, Y. You, T. Luo, X. M. Jia, and X. Lin. 2014. C-type lectin receptor dectin-3 mediates trehalose 6,6′-dimycolate (TDM)-induced Mincle expression through CARD9/Bcl10/MALT1-dependent nuclear factor (NF)-κB activation. *J. Biol. Chem.* 289: 30052–30062.
23. Kingeter, L. M., and X. Lin. 2012. C-type lectin receptor-induced NF-κB activation in innate immune and inflammatory responses. *Cell. Mol. Immunol.* 9: 105–112.
24. Sato, K., X. L. Yang, T. Yudate, J. S. Chung, J. Wu, K. Luby-Phelps, R. P. Kimberly, D. Underhill, P. D. Cruz, Jr., and K. Ariizumi. 2006. Dectin-2 is a pattern recognition receptor for fungi that couples with the Fc receptor gamma chain to induce innate immune responses. *J. Biol. Chem.* 281: 38854–38866.
25. Yamasaki, S., E. Ishikawa, M. Sakuma, H. Hara, K. Ogata, and T. Saito. 2008. Mincle is an ITAM-coupled activating receptor that senses damaged cells. *Nat. Immunol.* 9: 1179–1188.
26. Underhill, D. M., E. Rossnagle, C. A. Lowell, and R. M. Simmons. 2005. Dectin-1 activates Syk tyrosine kinase in a dynamic subset of macrophages for reactive oxygen production. *Blood* 106: 2543–2550.
27. Rogers, N. C., E. C. Slack, A. D. Edwards, M. A. Nolte, O. Schulz, E. Schweighoffer, D. L. Williams, S. Gordon, V. L. Tybulewicz, G. D. Brown, and C. Reis e Sousa. 2005. Syk-dependent cytokine induction by Dectin-1 reveals a novel pattern recognition pathway for C type lectins. *Immunity* 22: 507–517.
28. Robinson, M. J., F. Osorio, M. Rosas, R. P. Freitas, E. Schweighoffer, O. Gross, J. S. Verbeek, J. Ruland, V. Tybulewicz, G. D. Brown, et al. 2009. Dectin-2 is a Syk-coupled pattern recognition receptor crucial for Th17 responses to fungal infection. *J. Exp. Med.* 206: 2037–2051.
29. Deng, Z., S. Ma, H. Zhou, A. Zang, Y. Fang, T. Li, H. Shi, M. Liu, M. Du, P. R. Taylor, et al. 2015. Tyrosine phosphatase SHP-2 mediates C-type lectin receptor-induced activation of the kinase Syk and anti-fungal TH17 responses. *Nat. Immunol.* 16: 642–652.
30. Romani, L. 2004. Immunity to fungal infections. *Nat. Rev. Immunol.* 4: 1–23.
31. Hoving, J. C., G. J. Wilson, and G. D. Brown. 2014. Signalling C-type lectin receptors, microbial recognition and immunity. *Cell. Microbiol.* 16: 185–194.
32. Brown, G. D., J. Herre, D. L. Williams, J. A. Willment, A. S. Marshall, and S. Gordon. 2003. Dectin-1 mediates the biological effects of beta-glucans. *J. Exp. Med.* 197: 1119–1124.
33. Ishikawa, E., T. Ishikawa, Y. S. Morita, K. Toyonaga, H. Yamada, O. Takeuchi, T. Kinoshita, S. Akira, Y. Yoshikai, and S. Yamasaki. 2009. Direct recognition of the mycobacterial glycolipid, trehalose dimycolate, by C-type lectin Mincle. *J. Exp. Med.* 206: 2879–2888.
34. Mossalayi, M. D., N. Paul-Eugène, F. Ouaaz, M. Arock, J. P. Kolb, E. Kilchherr, P. Debré, and B. Dugas. 1994. Involvement of Fc epsilon RII/CD23 and L-arginine-dependent pathway in IgE-mediated stimulation of human monocyte functions. *Int. Immunol.* 6: 931–934.
35. Delespesse, G., U. Suter, D. Mossalayi, B. Bettler, M. Sarfati, H. Hofstetter, E. Kilcherr, P. Debre, and A. Dalloul. 1991. Expression, structure, and function of the CD23 antigen. *Adv. Immunol.* 49: 149–191.
36. Arock, M., L. Le Goff, P. A. Bécherel, B. Dugas, P. Debré, and M. D. Mossalayi. 1994. Involvement of Fc epsilon RII/CD23 and L-arginine dependent pathway in IgE-mediated activation of human eosinophils. *Biochem. Biophys. Res. Commun.* 203: 265–271.
37. Cheng, L. E., Z. E. Wang, and R. M. Locksley. 2010. Murine B cells regulate serum IgE levels in a CD23-dependent manner. *J. Immunol.* 185: 5040–5047.
38. Gonzalez-Molina, A., and H. L. Spiegelberg. 1976. Binding of IgE myeloma proteins to human cultured lymphoblastoid cells. *J. Immunol.* 117: 1838–1845.
39. Bonnefoy, J. Y., S. Lecoanet-Henchoz, J. F. Gauchat, P. Graber, J. P. Aubry, P. Jeannin, and C. Plater-Zyberk. 1997. Structure and functions of CD23. *Int. Rev. Immunol.* 16: 113–128.
40. Mossalayi, M. D., I. Vouldoukis, M. Mamani-Matsuda, T. Kauss, J. Guillon, J. Maugein, D. Moynet, J. Rambert, V. Desplat, D. Mazier, et al. 2009. CD23 mediates antimycobacterial activity of human macrophages. *Infect. Immun.* 77: 5537–5542.
41. Vouldoukis, I., V. Riveros-Moreno, B. Dugas, F. Ouaaz, P. Bécherel, P. Debré, S. Moncada, and M. D. Mossalayi. 1995. The killing of *Leishmania* major by human macrophages is mediated by nitric oxide induced after ligation of the Fc epsilon RII/CD23 surface antigen. *Proc. Natl. Acad. Sci. USA* 92: 7804–7808.
42. Zhao, X., Y. Guo, C. Jiang, Q. Chang, S. Zhang, T. Luo, B. Zhang, X. Jia, M. C. Hung, C. Dong, and X. Lin. 2017. JNK1 negatively controls antifungal innate immunity by suppressing CD23 expression. *Nat. Med.* 23: 337–346.
43. Bisgaard, L. S., C. K. Mogensen, A. Rosendahl, H. Cucak, L. B. Nielsen, S. E. Rasmussen, and T. X. Pedersen. 2016. Bone marrow-derived and peritoneal macrophages have different inflammatory response to oxLDL and M1/M2 marker expression - implications for atherosclerosis research. *Sci. Rep.* 6: 35234.
44. Goodridge, H. S., C. N. Reyes, C. A. Becker, T. R. Katsumoto, J. Ma, A. J. Wolf, N. Bose, A. S. Chan, A. S. Magee, M. E. Danielson, et al. 2011. Activation of the innate immune receptor Dectin-1 upon formation of a 'phagocytic synapse'. *Nature* 472: 471–475.
45. Brown, G. D. 2011. Innate antifungal immunity: the key role of phagocytes. *Annu. Rev. Immunol.* 29: 1–21.
46. Underhill, D. M., and E. Pearlman. 2015. Immune interactions with pathogenic and commensal fungi: a two-way street. *Immunity* 43: 845–858.
47. Wüthrich, M., G. S. Deepe, Jr., and B. Klein. 2012. Adaptive immunity to fungi. *Annu. Rev. Immunol.* 30: 115–148.
48. Rambert, J., M. Mamani-Matsuda, D. Moynet, P. Dubus, V. Desplat, T. Kauss, J. Dehais, T. Schaeverbeke, K. Ezzedine, D. Malvy, et al. 2009. Molecular blocking of CD23 supports its role in the pathogenesis of arthritis. *PLoS One* 4: e4834.
49. Richards, M. L., D. H. Katz, and F. T. Liu. 1991. Complete genomic sequence of the murine low affinity Fc receptor for IgE. Demonstration of alternative transcripts and conserved sequence elements. *J. Immunol.* 147: 1067–1074.
50. Conrad, D. H., K. A. Campbell, W. C. Bartlett, C. M. Squire, and S. E. Dierks. 1994. Structure and function of the low affinity IgE receptor. *Adv. Exp. Med. Biol.* 347: 17–30.
51. Gon, Y., and J. Yodoi. 1996. Low affinity Fc receptor for IgE (Fc epsilon R II/CD23). *Nihon Rinsho* 54: 456–460.
52. Kijimoto-Ochiai, S. 2002. CD23 (the low-affinity IgE receptor) as a C-type lectin: a multidomain and multifunctional molecule. *Cell. Mol. Life Sci.* 59: 648–664.
53. Jablonski, K. A., S. A. Amici, L. M. Webb, J. D. Ruiz-Rosado, P. G. Popovich, S. Partida-Sanchez, and M. Guerau-de-Arellano. 2015. Novel markers to delineate murine M1 and M2 macrophages. *PLoS One* 10: e0145342.
54. Vouldoukis, I., D. Mazier, D. Moynet, D. Thiolat, D. Malvy, and M. D. Mossalayi. 2011. IgE mediates killing of intracellular *Toxoplasma gondii* by human macrophages through CD23-dependent, interleukin-10 sensitive pathway. *PLoS One* 6: e18289.
55. Vonk, A. G., C. W. Wieland, M. G. Netea, and B. J. Kullberg. 2002. Phagocytosis and intracellular killing of *Candida albicans* blastoconidia by neutrophils and macrophages: a comparison of different microbiological test systems. *J. Microbiol. Methods* 49: 55–62.
56. Wirnsberger, G., F. Zwolanek, T. Asaoka, I. Kozieradzki, L. Tortola, R. A. Wimmer, A. Kavirayani, F. Fresser, G. Baier, W. Y. Langdon, et al. 2016. Inhibition of CBLB protects from lethal *Candida albicans* sepsis. *Nat. Med.* 22: 915–923.
57. Romero-Puertas, M. C., and L. M. Sandalio. 2016. Nitric oxide level is self-regulating and also regulates its ROS partners. *Front. Plant Sci.* 7: 316.
58. Chan, E. D., K. R. Morris, J. T. Belisle, P. Hill, L. K. Remigio, P. J. Brennan, and D. W. Riches. 2001. Induction of inducible nitric oxide synthase-NO* by lipoarabinomannan of *Mycobacterium tuberculosis* is mediated by MEK1-ERK, MKK7-JNK, and NF-kappaB signaling pathways. *Infect. Immun.* 69: 2001–2010.
59. Nishiya, T., T. Uehara, H. Edamatsu, Y. Kaziro, H. Itoh, and Y. Nomura. 1997. Activation of Stat1 and subsequent transcription of inducible nitric oxide synthase gene in C6 glioma cells is independent of interferon-gamma-induced MAPK activation that is mediated by p21ras. *FEBS Lett.* 408: 33–38.
60. Bhat, N. R., P. Zhang, J. C. Lee, and E. L. Hogan. 1998. Extracellular signal-regulated kinase and p38 subgroups of mitogen-activated protein kinases regulate inducible nitric oxide synthase and tumor necrosis factor-alpha gene expression in endotoxin-stimulated primary glial cultures. *J. Neurosci.* 18: 1633–1641.
61. Kamijo, R., H. Harada, T. Matsuyama, M. Bosland, J. Gerecitano, D. Shapiro, J. Le, S. I. Koh, T. Kimura, S. J. Green, et al. 1994. Requirement for transcription factor IRF-1 in NO synthase induction in macrophages. *Science* 263: 1612–1615.
62. Saijo, S., N. Fujikado, T. Furuta, S. H. Chung, H. Kotaki, K. Seki, K. Sudo, S. Akira, Y. Adachi, N. Ohno, et al. 2007. Dectin-1 is required for host defense against *Pneumocystis carinii* but not against *Candida albicans*. *Nat. Immunol.* 8: 39–46.
63. Huang, J. H., C. Y. Lin, S. Y. Wu, W. Y. Chen, C. L. Chu, G. D. Brown, C. P. Chuu, and B. A. Wu-Hsieh. 2015. CR3 and Dectin-1 collaborate in macrophage cytokine response through association on lipid rafts and activation of Syk-JNK-AP-1 pathway. *PLoS Pathog.* 11: e1004985.
64. Marakalala, M. J., S. Vautier, J. Potrykus, L. A. Walker, K. M. Shepardson, A. Hopke, H. M. Mora-Montes, A. Kerrigan, M. G. Netea, G. I. Murray, et al. 2013. Differential adaptation of *Candida albicans* in vivo modulates immune recognition by Dectin-1. *PLoS Pathog.* 9: e1003315
65. Wang, H., M. Li, T. Lerksuthirat, B. Klein, and M. Wüthrich. 2015. The C-Type lectin receptor MCL mediates vaccine-induced immunity against infection with blastomyces dermatitidis. *Infect. Immun.* 84: 635–642.
66. Ishikawa, T., F. Itoh, S. Yoshida, S. Saijo, T. Matsuzawa, T. Gonoi, T. Saito, Y. Okawa, N. Shibata, T. Miyamoto, and S. Yamasaki. 2013. Identification of distinct ligands for the C-type lectin receptors Mincle and Dectin-2 in the pathogenic fungus Malassezia. *Cell Host Microbe* 13: 477–488.

67. Lee, S. J., N. Y. Zheng, M. Clavijo, and M. C. Nussenzweig. 2003. Normal host defense during systemic candidiasis in mannose receptor-deficient mice. *Infect. Immun.* 71: 437–445.
68. Netea, M. G., N. A. Gow, C. A. Munro, S. Bates, C. Collins, G. Ferwerda, R. P. Hobson, G. Bertram, H. B. Hughes, T. Jansen, et al. 2006. Immune sensing of *Candida albicans* requires cooperative recognition of mannans and glucans by lectin and Toll-like receptors. *J. Clin. Invest.* 116: 1642–1650.
69. van Kooyk, Y., and T. B. Geijtenbeek. 2003. DC-SIGN: escape mechanism for pathogens. *Nat. Rev. Immunol.* 3: 697–709.
70. Serrano-Gómez, D., A. Domínguez-Soto, J. Ancochea, J. A. Jimenez-Heffernan, J. A. Leal, and A. L. Corbí. 2004. Dendritic cell-specific intercellular adhesion molecule 3-grabbing nonintegrin mediates binding and internalization of *Aspergillus fumigatus* conidia by dendritic cells and macrophages. *J. Immunol.* 173: 5635–5643.
71. Taylor, P. R., G. D. Brown, J. Herre, D. L. Williams, J. A. Willment, and S. Gordon. 2004. The role of SIGNR1 and the beta-glucan receptor (dectin-1) in the nonopsonic recognition of yeast by specific macrophages. *J. Immunol.* 172: 1157–1162.
72. Jouault, T., M. El Abed-El Behi, M. Martínez-Esparza, L. Breuilh, P. A. Trinel, M. Chamaillard, F. Trottein, and D. Poulain. 2006. Specific recognition of *Candida albicans* by macrophages requires galectin-3 to discriminate *Saccharomyces cerevisiae* and needs association with TLR2 for signaling. *J. Immunol.* 177: 4679–4687.
73. Majer, O., C. Bourgeois, F. Zwolanek, C. Lassnig, D. Kerjaschki, M. Mack, M. Müller, and K. Kuchler. 2012. Type I interferons promote fatal immunopathology by regulating inflammatory monocytes and neutrophils during candida infections. *PLoS Pathog.* 8: e1002811.
74. Mircescu, M. M., L. Lipuma, N. van Rooijen, E. G. Pamer, and T. M. Hohl. 2009. Essential role for neutrophils but not alveolar macrophages at early time points following *Aspergillus fumigatus* infection. *J. Infect. Dis.* 200: 647–656.
75. Borregaard, N. 2010. Neutrophils, from marrow to microbes. *Immunity* 33: 657–670.
76. Lionakis, M. S., J. K. Lim, C. C. Lee, and P. M. Murphy. 2011. Organ-specific innate immune responses in a mouse model of invasive candidiasis. *J. Innate Immun.* 3: 180–199.
77. Green, S. J., R. M. Crawford, J. T. Hockmeyer, M. S. Meltzer, and C. A. Nacy. 1990. *Leishmania* major amastigotes initiate the L-arginine-dependent killing mechanism in IFN-gamma-stimulated macrophages by induction of tumor necrosis factor-alpha. *J. Immunol.* 145: 4290–4297.
78. Chan, J., Y. Xing, R. S. Magliozzo, and B. R. Bloom. 1992. Killing of virulent *Mycobacterium tuberculosis* by reactive nitrogen intermediates produced by activated murine macrophages. *J. Exp. Med.* 175: 1111–1122.
79. Vazquez-Torres, A., J. Jones-Carson, T. Warner, and E. Balish. 1995. Nitric oxide enhances resistance of SCID mice to mucosal candidiasis. *J. Infect. Dis.* 172: 192–198.
80. Newman, S. L., and A. Holly. 2001. *Candida albicans* is phagocytosed, killed, and processed for antigen presentation by human dendritic cells. *Infect. Immun.* 69: 6813–6822.